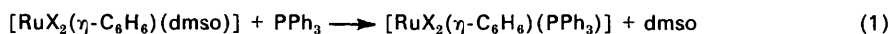


Mechanisms of Organometallic Substitution Reactions. Part 4.† Kinetics of Replacement of Dimethyl Sulphoxide (dmsO) from $[\text{RuX}_2(\eta\text{-C}_6\text{H}_6)(\text{dmsO})]$ ($\text{X} = \text{Cl}$ or Br) Complexes by Triphenylphosphine

By Christopher M. Carr, Daphne M. Davies, Marian Gower, Leon A. P. Kane-Maguire,* and Dwight A. Sweigart, Chemistry Department, University College Cardiff, P.O. Box 78, Cardiff CF1 1XL

A kinetic study has been undertaken of the replacement of dimethyl sulphoxide (dmsO) in $[\text{RuX}_2(\eta\text{-C}_6\text{H}_6)(\text{dmsO})]$ ($\text{X} = \text{Cl}$ or Br) by triphenylphosphine in both dmsO and 1,2-dichloroethane as solvent [equation (1)]. For the

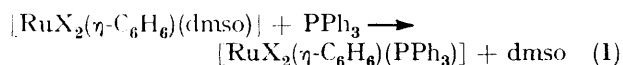


relatively slow reactions in dmsO the rate law, $\text{rate} = k[\text{complex}][\text{PPh}_3]$, is observed. However, a stopped-flow kinetic investigation of the rapid reactions in 1,2-dichloroethane supports a rate law of the form: $\text{rate} = k_1k_2[\text{complex}][\text{PPh}_3]/(k_{-1}[\text{dmsO}] + k_2[\text{PPh}_3])$. For both solvents a mechanism is proposed involving initial dissociation (k_1) of the dmsO ligand generating the co-ordinatively unsaturated intermediates, $[\text{RuX}_2(\eta\text{-C}_6\text{H}_6)]$, which may then either recombine (k_{-1}) with dmsO to regenerate the starting complexes or add a PPh_3 ligand irreversibly (k_2) to yield the observed products.

A WIDE variety of π -arene complexes of ruthenium(II) have been reported¹⁻¹⁰ in recent years. This interest has been stimulated in part because of their catalytic activity in olefin hydrogenation^{2,9} and ring-opening polymerisation reactions.¹¹ For example, the ability of the dimer $[\{\text{RuCl}_2(\eta\text{-C}_6\text{H}_6)\}_2]$ (1) to catalyse the hydrogenation of pent-1-ene to pentane is reported² to be similar to that of the well known catalyst $[\text{RuCl}_2(\text{PPh}_3)_3]$. The complex formed by (1) in dimethyl sulphoxide (dmsO) has been isolated² and characterised as $[\text{RuX}_2(\eta\text{-C}_6\text{H}_6)(\text{dmsO})]$ (2; $\text{X} = \text{Cl}$). This monomer has itself been successfully used² to hydrogenate maleic acid to fumaric acid in aqueous solution at room temperature.

Further interest arises from the report³ that a variety of nucleophiles such as CN^- , OH^- , and H^- react with (1) in dmsO to give cyclohexadienyl complexes. Similarly, the π -arene rings in $[\text{Ru}(\eta\text{-arene})_2]^{2+}$ cations are also susceptible to nucleophilic addition.¹²

Since ligand substitution at ruthenium(II) must be an integral step in olefin hydrogenation and a potential alternative pathway to nucleophilic addition at the π -arene ring, quantitative mechanistic information on ligand substitution is fundamental to our understanding of both types of processes. In view of the paucity of such data, we wish to report a detailed kinetic investigation of the reactions of (2; $\text{X} = \text{Cl}$ or Br) with triphenylphosphine to yield $[\text{RuX}_2(\eta\text{-C}_6\text{H}_6)(\text{PPh}_3)]$ (3), equation (1). Studies in dmsO and 1,2-dichloroethane



solvents reveal that these ligand substitutions are dissociative in character.

EXPERIMENTAL

Materials.—The complexes $[\text{RuX}_2(\eta\text{-C}_6\text{H}_6)(\text{dmsO})]$ ($\text{X} = \text{Cl}$ or Br) were prepared from the related dimers $[\{\text{RuX}_2-$

$(\eta\text{-C}_6\text{H}_6)\}_2]$ using published procedures.^{2,3} They were recrystallised from aqueous ethanol at -10°C in *ca.* 50% yield (Found: C, 29.6; H, 3.7; Cl, 23.0. Calc. for $\text{C}_8\text{H}_{12}\text{Cl}_2\text{ORuS}$: C, 29.3; H, 3.7; Cl, 21.7%. Found: C, 23.0; H, 2.8; Br, 40.4. Calc. for $\text{C}_8\text{H}_{12}\text{Br}_2\text{ORuS}$: C, 23.0; H, 2.9; Br, 38.5%). The u.v.-visible spectrum of the chloro-complex in dmsO solvent exhibited a maximum at 372 nm ($\epsilon = 950 \text{ dm}^3 \text{ mol}^{-1} \text{ cm}^{-1}$). The bromo-compound showed a band at 378 nm ($\epsilon = 1090 \text{ dm}^3 \text{ mol}^{-1} \text{ cm}^{-1}$). Both complexes, as expected, showed molar conductivities near zero a few minutes after dissolution in dmsO.

An attempt to prepare the unknown $[\text{RuI}_2(\eta\text{-C}_6\text{H}_6)(\text{dmsO})]$ complex from $[\{\text{RuI}_2(\eta\text{-C}_6\text{H}_6)\}_2]$ using an analogous procedure to those above was unsuccessful.

The product $[\text{RuCl}_2(\eta\text{-C}_6\text{H}_6)(\text{PPh}_3)]$ was also prepared by a published method³ (Found: C, 57.2; H, 4.5; Cl, 13.5. Calc. for $\text{C}_{24}\text{H}_{21}\text{Cl}_2\text{PRu}$: C, 56.3; H, 4.1; Cl, 13.9%). It exhibited a visible band in 1,2-dichloroethane at 370 nm ($\epsilon = 2360 \text{ dm}^3 \text{ mol}^{-1} \text{ cm}^{-1}$).

1,2-Dichloroethane solvent was distilled in bulk and stored over molecular sieves. Dimethyl sulphoxide was purified by standing overnight over barium oxide, filtering, and distilling under vacuum (10^{-2} Torr, \dagger 30°C).

Spectroscopic Studies.—U.v.-visible spectra were recorded on a Beckman DK2A spectrophotometer using matched 1-cm silica cells. Molar conductivities were measured using a Pye Unicam model E7566/2 conductivity bridge.

Kinetic Studies.—All reactions were studied under pseudo-first-order conditions using a large excess of nucleophile. The reactions of (2) with PPh_3 in dmsO solvent were slow enough to follow by conventional techniques. Solutions of PPh_3 in dmsO (5 cm³) and starting complex (*ca.* 2 mg) in dmsO (5 cm³) were freshly prepared and thermostatted in a bath at the desired temperature ($\pm 0.1^\circ\text{C}$) for 10 min. The solutions were then mixed, and an aliquot rapidly transferred to a 1-cm silica cell in the thermostatted cell block of a Beckman DK2A spectrophotometer. Spectra were recorded at appropriate intervals, and both reactions monitored by following the growth of the $[\text{RuX}_2(\eta\text{-C}_6\text{H}_6)(\text{PPh}_3)]$ (3; $\text{X} = \text{Cl}$ or Br) product bands at 370 and 378 nm, respectively.

The analogous reactions in 1,2-dichloroethane solvent

† Part 3, M. Gower and L. A. P. Kane-Maguire, *Inorg. Chim. Acta* 1979, **37**, 79.

‡ Throughout this paper: 1 Torr = (101325/760) Pa.

(containing various amounts of added dmsO) were rapid, and were therefore monitored using a thermostatted stopped-flow spectrophotometer. Fresh solutions of the reactants were allowed to equilibrate at the desired temperature ($\pm 0.1^\circ\text{C}$) for 10 min prior to mixing. A large increase in absorbance occurred at 370 nm ($X = \text{Cl}$) and 378 nm ($X = \text{Br}$) during the reactions. Reaction traces were stored on a Tektronix 564 oscilloscope fitted with a log converter for direct absorbance readout, and photographed on 35 mm film. Each run was carried out in triplicate.

For all reactions, pseudo-first-order rate constants, k_{obs} , were calculated from the slopes of plots of $\log(A_\infty - A_t)$ against time. Such plots were generally linear for 75–90% completion of reaction.

Values of $\Delta H^\ddagger_{\text{obs}}$ in dmsO solvent were obtained from the gradients of Arrhenius plots of $\log k_{\text{obs}}$, ($[\text{PPh}_3]$ constant) versus $1/T$. Standard errors of estimation were obtained from a least-squares treatment. Associated $\Delta S^\ddagger_{\text{obs}}$ values were calculated after multiplying the apparent second-order rate constants, k , by 14.1 mol dm^{-3} to eliminate the dmsO solvent term.

RESULTS AND DISCUSSION

(a) *Dimethyl Sulphoxide Solvent.*—Although reaction (1) is well established in dmsO solvent, spectroscopic and conductometric studies were carried out on the starting materials and reported products to check for potential side reactions involving halide displacement by dmsO. In the absence of PPh_3 , both $[\text{RuX}_2(\eta\text{-C}_6\text{H}_6)(\text{dmsO})]$ complexes showed near-zero molar conductivities as expected for the first few minutes after dissolving in dmsO (see Experimental section). However, in both cases the conductivity subsequently increased slowly with time, Λ_M maximising at $11\text{--}14 \text{ }\Omega^{-1} \text{ cm}^2 \text{ mol}^{-1}$ overnight. A concomitant slow decrease in absorbance at *ca.* 345 nm was observed. This behaviour suggests slow, partial displacement of co-ordinated halide ion from the starting complexes by dmsO.

However, these background reactions in dmsO are generally too slow to interfere significantly with kinetic investigation of reactions (1), as evidenced by the sharp isosbestic points observed at *ca.* 340 nm ($X = \text{Cl}$) and *ca.* 350 nm ($X = \text{Br}$) throughout the slower reactions (1) [Figure 1(a) and (b)]. The absence of such background interference is also indicated by the fact that plots of k_{obs} versus $[\text{PPh}_3]$ for both reactions (1) in dmsO pass through the origin (Figure 2).

Similarly, experiments showed that the products $[\text{RuX}_2(\eta\text{-C}_6\text{H}_6)(\text{PPh}_3)]$ ($X = \text{Cl}$ or Br), while non-electrolytes in dmsO at zero time, slowly increased their conductivity to *ca.* $16 \text{ }\Omega^{-1} \text{ cm}^2 \text{ mol}^{-1}$ after 40 h. This value is the same as that of the known 1:1 electrolyte *trans*- $[\text{CoCl}_2(\text{en})_2]\text{Cl}$ in dmsO, suggesting that slow displacement of halide by dmsO has again occurred leading perhaps to $[\text{RuX}(\eta\text{-C}_6\text{H}_6)(\text{dmsO})(\text{PPh}_3)]$ species. Crude k_{obs} values of $4.6 \times 10^{-6} \text{ s}^{-1}$ ($X = \text{Cl}$) and $1.7 \times 10^{-5} \text{ s}^{-1}$ ($X = \text{Br}$) were estimated for these decompositions at 30°C using u.v.-visible spectroscopy. Since these rate constants are in most cases much slower than the k_{obs} values obtained for reactions (1), little interference is expected from these subsequent decompositions. This

is confirmed by the fact that the final *in situ* product from reaction (1; $X = \text{Cl}$) has, within experimental error, the same absorption coefficient at 370 nm as an independently prepared pure sample of (3; $X = \text{Cl}$).

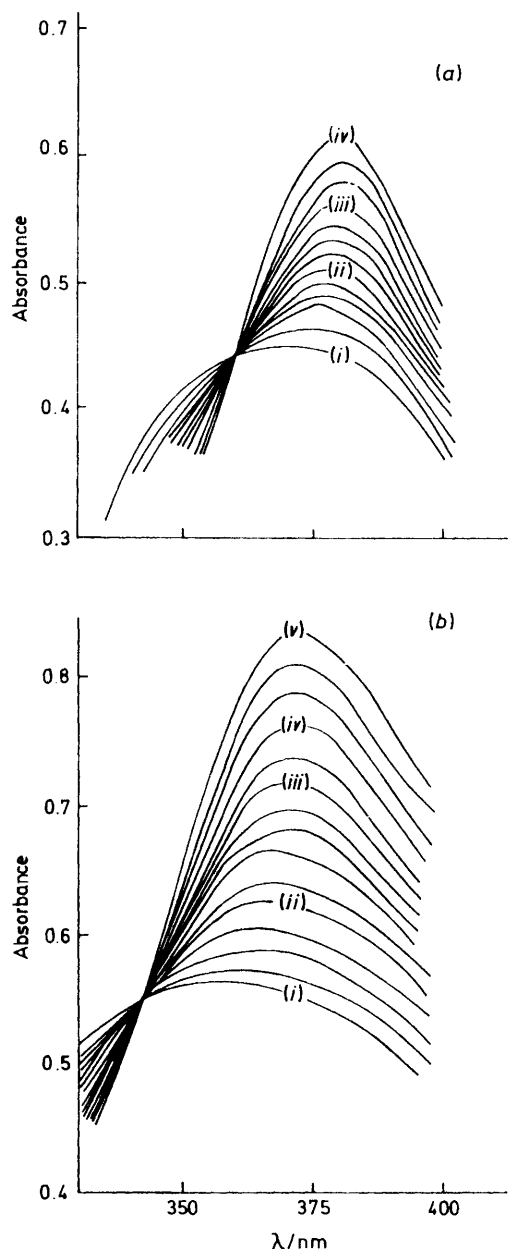


FIGURE 1 U.v.-visible spectral changes during the reaction (dmsO, 30°C) of (a) $[\text{RuBr}_2(\eta\text{-C}_6\text{H}_6)(\text{dmsO})]$ with PPh_3 ($10^{-2} \text{ mol dm}^{-3}$) after (i) 5, (ii) 10, (iii) 14, and (iv) 35 min; and (b) $[\text{RuCl}_2(\eta\text{-C}_6\text{H}_6)(\text{dmsO})]$ with PPh_3 ($7.5 \times 10^{-3} \text{ mol dm}^{-3}$) after (i) 1, (ii) 3, (iii) 5.67, (iv) 8, and (v) 18 min

Kinetic results for reactions (1; $X = \text{Cl}$ or Br) in dmsO are summarised in Tables 1 and 2, respectively. The linearity of plots of k_{obs} versus $[\text{PPh}_3]$ for both complexes (Figure 2) indicates the rate law (2). At 30°C the chloro-complex reacts about three times faster than the analogous bromo-compound. These relatively

$$\text{Rate} = k[\text{complex}][\text{PPh}_3] = k_{\text{obs}}[\text{complex}] \quad (2)$$

TABLE 1

Kinetic results for the reaction of $[\text{RuCl}_2(\eta\text{-C}_6\text{H}_6)(\text{dmsO})]$ with PPh_3 in dmsO *

$\theta_c/^\circ\text{C}$	$10^3[\text{PPh}_3]/\text{mol dm}^{-3}$	$10^3k_{\text{obs.}}/\text{s}^{-1}$
30.0	3.0	1.64
30.0	5.0	3.00
30.0	7.5	3.68
30.0	10.0	5.43
30.0	15.0	7.59
30.0	20.0	10.9
35.8	5.0	4.36
38.6	5.0	6.29
44.4	5.0	8.86
46.3	5.0	11.8
50.3	5.0	16.2

* $[\text{Ru}] = 5.0 \times 10^{-4} \text{ mol dm}^{-3}$.

TABLE 2

Kinetic results for the reaction of $[\text{RuBr}_2(\eta\text{-C}_6\text{H}_6)(\text{dmsO})]$ with PPh_3 in dmsO ^a

$\theta_c/^\circ\text{C}$	$10^3[\text{PPh}_3]/\text{mol dm}^{-3}$	$10^3k_{\text{obs.}}/\text{s}^{-1}$
30.0	2.56	0.49 ^b
30.0	3.44	0.71 ^b
30.0	5.00	0.92
30.0	10.0	1.79 ^c
30.0	12.5	2.67
30.0	15.0	3.05
30.0	20.0	3.60
30.0	25.0	4.83
25.5	15.0	2.08
35.0	15.0	4.81
40.0	15.0	7.78
45.2	15.0	11.4
49.8	15.0	17.8

^a $[\text{Ru}] = 5.0 \times 10^{-4} \text{ mol dm}^{-3}$, unless otherwise stated.^b $[\text{Ru}] = 3.6 \times 10^{-4} \text{ mol dm}^{-3}$. ^c $[\text{Ru}] = 7.4 \times 10^{-4} \text{ mol dm}^{-3}$.

similar rates for the chloro- and bromo-complexes are reflected in their similar $\Delta H^\ddagger_{\text{obs.}}$ and $\Delta S^\ddagger_{\text{obs.}}$ values (Table 3).

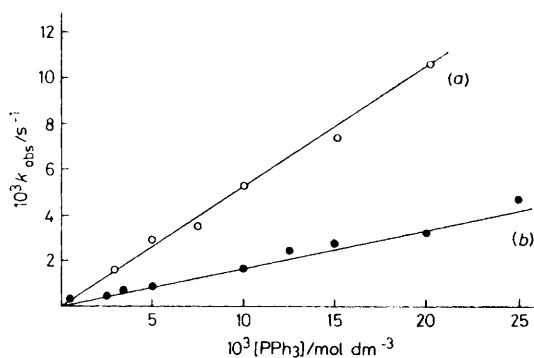


FIGURE 2 Dependence of $k_{\text{obs.}}$ on $[\text{PPh}_3]$ for the reactions of PPh_3 in dmsO at 30°C with (a) $[\text{RuCl}_2(\eta\text{-C}_6\text{H}_6)(\text{dmsO})]$ and (b) $[\text{RuBr}_2(\eta\text{-C}_6\text{H}_6)(\text{dmsO})]$

The observation of rate law (2) might suggest an associative mechanism for processes (1) in dmsO. However, subsequent kinetic studies in 1,2-dichloroethane solvent clearly indicate that these reactions are dissociative in character, and that equation (2) observed in dmsO is a limiting case of a more general rate law.

(b) 1,2-Dichloroethane Solvent.—Kinetic results for reactions (1) at 19°C in 1,2-dichloroethane solvent containing various amounts of added dmsO are collected in

Tables 4 and 5. In each case the added dmsO was sufficient to maintain $[\text{dmsO}]$ effectively constant through-

TABLE 3

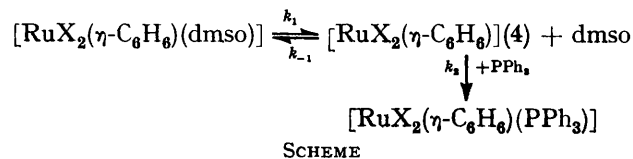
Rate and activation parameters for the reactions of $[\text{RuX}_2(\eta\text{-C}_6\text{H}_6)(\text{dmsO})]$ ($\text{X} = \text{Cl}$ or Br) with PPh_3 in dmsO ^a

X	$k_{30} \text{ } ^\circ\text{C} \text{ } ^b/$ $\text{dm}^3 \text{ mol}^{-1} \text{ s}^{-1}$	$\Delta H^\ddagger_{\text{obs.}}/$ kJ mol^{-1}	$\Delta S^\ddagger_{\text{obs.}}/$ $\text{J K}^{-1} \text{ mol}^{-1}$
Cl	0.529(0.021)	66(4)	-11(12)
Br	0.190(0.007)	69(3)	-9(10)

^a Values in parentheses are estimated standard deviations.^b From least-squares analyses of results in Tables 1 and 2.

out the reactions, despite the release of dmsO ligand. Plots of $k_{\text{obs.}}$ versus $[\text{PPh}_3]$ at each dmsO concentration are given in Figure 3(a) for the complex ($\text{X} = \text{Br}$). Interestingly, while $k_{\text{obs.}}$ shows a linear dependence on $[\text{PPh}_3]$ at low phosphine concentrations, the individual plots become curved at higher $[\text{PPh}_3]$ and appear to tend towards a limiting value. Similar behaviour is exhibited by the complex ($\text{X} = \text{Cl}$).

A mechanism consistent with all the experimental results is outlined in the Scheme. This mechanism involves initial dissociation (k_1) of the dmsO ligand



generating the co-ordinatively unsaturated intermediate (4), which may then either recombine (k_{-1}) with dmsO to regenerate the starting complex or add (k_2) a PPh_3 ligand irreversibly to yield the observed product (3).

Assuming a steady-state concentration of intermediate (4), this mechanism leads to the general expression (3) for $k_{\text{obs.}}$. Under the limiting condition

$$k_{\text{obs.}} = k_1 k_2 [\text{PPh}_3] / (k_{-1} [\text{dmsO}] + k_2 [\text{PPh}_3]) \quad (3)$$

$$k_{\text{obs.}} = k_1 k_2 [\text{PPh}_3] / k_{-1} [\text{dmsO}] \quad (4)$$

$k_{-1} [\text{dmsO}] \gg k_2 [\text{PPh}_3]$, this expression simplifies to equation (4) which explains the linear dependence of $k_{\text{obs.}}$ on $[\text{PPh}_3]$ found for both complexes in 1,2-dichloroethane solvent at low phosphine concentrations [see Figure 3(a)]. Also consistent with equation (4) is the marked dependence of $k_{\text{obs.}}$ for both complexes on $[\text{dmsO}]$, e.g. for $[\text{RuBr}_2(\eta\text{-C}_6\text{H}_6)(\text{dmsO})]$ with $[\text{PPh}_3] = 0.01 \text{ mol dm}^{-3}$, the run carried out with $[\text{dmsO}] = 0.7 \text{ mol dm}^{-3}$ is 365 times slower than that with $[\text{dmsO}] = 0.002 \text{ mol dm}^{-3}$ (Table 5).

On the other hand, when $k_2 [\text{PPh}_3] \gg k_{-1} [\text{dmsO}]$ the limiting equation (5) is expected. This explains the

$$k_{\text{obs.}} = k_1 \quad (5)$$

curvature towards limiting rates of the $k_{\text{obs.}}$ versus $[\text{PPh}_3]$ plots for both complexes at high phosphine concentrations [see Figure 3(a)]. The $k_{\text{obs.}}$ values in Tables 4 and 5 obtained in the absence of added dmsO and employing a large excess of phosphine ($[\text{PPh}_3] = 0.1 \text{ mol dm}^{-3}$) therefore refer to the dissociation rate constants,

k_1 , for the complexes ($X = \text{Cl}$ and Br) (ca. 10 and 5 s⁻¹, respectively).

Inversion of the general equation (3) leads to equation (6). The quantitative fit of the experimental results to

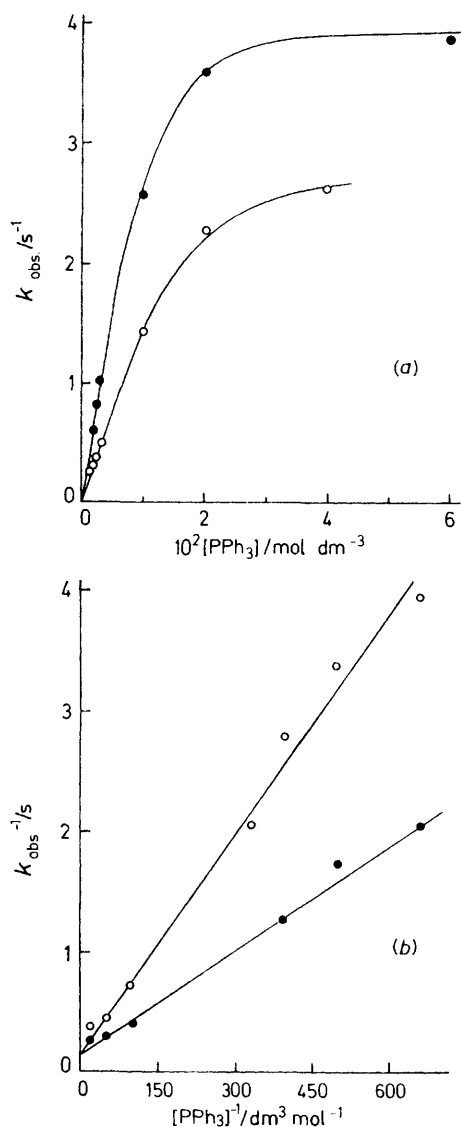


FIGURE 3 The reaction of $[\text{RuBr}_2(\eta\text{-C}_6\text{H}_6)](\text{dmsO})$ with PPh_3 in 1,2-dichloroethane at 19.0 °C: $[\text{dmsO}]$ added = 2.0×10^{-3} (●), and 5×10^{-3} mol dm⁻³ (○). (a) Dependence of k_{obs} on $[\text{PPh}_3]$; (b) plot of k_{obs}^{-1} versus $[\text{PPh}_3]^{-1}$

equation (6) is shown by the excellent linearity of plots of $1/k_{\text{obs}}$, versus $1/[\text{PPh}_3]$ (at constant $[\text{dmsO}]$) for each complex, Figure 3(b), and from the linear dependence

$$1/k_{\text{obs}} = 1/k_1 + k_{-1}[\text{dmsO}]/k_1k_2[\text{PPh}_3] \quad (6)$$

of the slopes on $[\text{dmsO}]$ (Table 6). The k_1 values calculated from the intercepts ($1/k_1$) of such plots agree within experimental error with the limiting k_{obs} values obtained above in the absence of added dmsO.

The above results indicate that dissociation (k_{-1}) of a dmsO ligand from the chloro-complex is about twice as fast as from the bromo-analogue at 19.0 °C in 1,2-di-

TABLE 4

Kinetic results for the reaction of $[\text{RuCl}_2(\eta\text{-C}_6\text{H}_6)](\text{dmsO})$ with PPh_3 in 1,2-dichloroethane *

$10^2[\text{dmsO}]/$ mol dm ⁻³	$10^2[\text{PPh}_3]/$ mol dm ⁻³	$k_{\text{obs.}}/\text{s}^{-1}$
0	5.0	10.5
0	10.0	10.8
0.24	0.25	1.96
0.24	0.50	3.01
0.24	1.25	3.70
0.24	2.50	5.35
0.64	0.15	0.663
0.64	0.25	1.14
0.64	0.40	1.53
0.64	0.80	2.63
0.64	1.25	3.80
0.64	2.50	4.63

* $\theta_c = 19.0$ °C; $[\text{Ru}] = 1.84 \times 10^{-4}$ mol dm⁻³.

chloroethane. In addition, combination of intercepts and slopes from the inverse plots such as Figure 3(b) provide the ratio k_{-1}/k_2 , which is a measure of the discrimination of the intermediate (4) between the potential nucleophiles dmsO and PPh_3 . This ratio is seen (Table 6) to be significantly larger for the bromo-complex.

In view of the results in dichloroethane, a dissociative mechanism for reactions (1) also seems highly probable in dmsO solvent. The linearity of the plots of k_{obs} against $[\text{PPh}_3]$ for both $X = \text{Cl}$ or Br complexes in dmsO (Figure 2) undoubtedly arises from the fact that the limiting condition $k_{-1}[\text{dmsO}] \gg k_2[\text{PPh}_3]$ holds over the entire phosphine concentration range employed, *i.e.* k_{obs} is given by equation (4). The very much lower k_{obs} values found for both complexes in dmsO compared with dichloroethane can be readily explained on the basis of the high value of $k_{-1}[\text{dmsO}]$ in equation (4) for the former solvent.

Interestingly, for the reaction of the bromo-complex with $[\text{PPh}_3] = 1.0 \times 10^{-2}$ mol dm⁻³ at 19.0 °C, the measured k_{obs} in dmsO of 5.0×10^{-4} s⁻¹ (Table 5) is very similar to the calculated k_{obs} value for '14.1 mol dm⁻³

TABLE 5

Kinetic results for the reaction of $[\text{RuBr}_2(\eta\text{-C}_6\text{H}_6)](\text{dmsO})$ with PPh_3 in 1,2-dichloroethane ^a

$10^2[\text{dmsO}]/$ mol dm ⁻³	$10^2[\text{PPh}_3]/$ mol dm ⁻³	$10^2k_{\text{obs.}}/\text{s}^{-1}$
0	10	508
0.20	0.15	49.6
0.20	0.20	58.3
0.20	0.25	80.0
0.20	0.30	101
0.20	1.00	257
0.20	2.00	358
0.20	6.00	385
0.50	0.15	25.8
0.50	0.20	29.8
0.50	0.25	36.2
0.50	0.30	49.4
0.50	1.00	142
0.50	2.00	228
0.50	4.00	264
28	0.50	1.02
70	0.50	0.542
70	1.00	0.704
1 410 ^b	1.00	0.050

^a $\theta_c = 19.0$ °C; $[\text{Ru}] = 3 \times 10^{-4}$ mol dm⁻³ ^b Pure dmsO solvent.

dmso in 1,2-dichloroethane', namely $ca. 4.7 \times 10^{-4} \text{ s}^{-1}$ [assuming equation (4) and using results in Tables 5 and 6]. This suggests (a) that the nature of the solvent has little effect on the rate constants, and (b) that pure dmso does indeed behave like a 14.1 mol dm⁻³ 'solution'.

TABLE 6

Parameters derived from plots of $1/k_{\text{obs}}$, versus $1/[\text{PPh}_3]$ for the reactions of $[\text{RuX}_2(\eta\text{-C}_6\text{H}_6)](\text{dmso})$ with PPh_3 in 1,2-dichloroethane at 19.0 °C^a

X	$10^2[\text{dmso}]/$ mol dm ⁻³	$10^3(\text{slope})^b$	k_{-1}/k_2
Cl	0.24	0.838 (0.076)	2.41
Cl	0.64	2.05 (0.06)	2.21
Br	0.20	2.86 (0.13)	8.43
Br	0.50	5.85 (0.32)	6.90

^a Values in parentheses are estimated standard deviations.

^b Slope = $k_{-1}[\text{dmso}]/k_1k_2$.

Assuming that the mechanism in the Scheme is followed in dmso, it should also be noted that the apparent second-order rate constants, k , in Table 3 refer to the ratio $k_1k_2/k_{-1}(\text{dmso})$, i.e. the $\Delta H_{\text{obs}}^\ddagger$ and $\Delta S_{\text{obs}}^\ddagger$ values are composite parameters.

We thank the S.R.C. for support.

[0/1368 Received, 4th September, 1980]

REFERENCES

- ¹ G. Winkhaus and H. Singer, *J. Organomet. Chem.*, 1967, **7**, 487.
- ² I. Ogata, R. Iwata, and Y. Ikeda, *Tetrahedron Lett.*, 1970, **34**, 3011.
- ³ R. A. Zelonka and M. C. Baird, *Can. J. Chem.*, 1972, **50**, 3063, and references therein.
- ⁴ M. A. Bennett, G. B. Robertson, and A. K. Smith, *J. Organomet. Chem.*, 1972, **43**, C41.
- ⁵ R. A. Zelonka and M. C. Baird, *J. Organomet. Chem.*, 1972, **44**, 383.
- ⁶ M. A. Bennett and A. K. Smith, *J. Chem. Soc., Dalton Trans.*, 1974, 233.
- ⁷ D. R. Robertson and T. A. Stephenson, *J. Organomet. Chem.*, 1976, **116**, C29.
- ⁸ D. R. Robertson and T. A. Stephenson, *J. Chem. Soc., Dalton Trans.*, 1978, 486, and references therein.
- ⁹ M. A. Bennett, T.-N. Huang, A. K. Smith, and T. W. Turney, *J. Chem. Soc., Chem. Commun.*, 1978, 582, and references therein.
- ¹⁰ M. A. Bennett and T. W. Matheson, *J. Organomet. Chem.*, 1979, **175**, 87, and references therein.
- ¹¹ L. Porri, P. Diversi, A. Lucherini, and R. Rossi, *Makromol. Chem.*, 1975, **176**, 3121.
- ¹² P. J. Domaille, S. D. Ittel, J. P. Jesson, and D. A. Sweigart, *Inorg. Chem.*, in the press.